The Journal of Immunology

Online Hemodiafiltration Inhibits Inflammation-Related Endothelial Dysfunction and Vascular Calcification of Uremic Patients Modulating miR-223 Expression in Plasma Extracellular Vesicles

Claudia Cavallari, Sergio Dellepiane, Valentina Fonsato, Davide Medica, Marita Marengo, Massimiliano Migliori, Alessandro D. Quercia, Adriana Pitino, Marco Formica, Vincenzo Panichi, Stefano Maffei, Luigi Biancone, Emanuele Gatti, Ciro Tetta, Giovanni Camussi and Vincenzo Cantaluppi

J Immunol published online 4 March 2019
http://www.jimmunol.org/content/early/2019/03/01/jimmunol.1800747

The Journal of Immunology is published twice each month by The American Association of Immunologists, Inc., 1451 Rockville Pike, Suite 650, Rockville, MD 20852

Print ISSN: 0022-1767 Online ISSN: 1550-6606.

Published March 4, 2019, doi:10.4049/jimmunol.1800747

Online Hemodiafiltration Inhibits Inflammation-Related Endothelial Dysfunction and Vascular Calcification of Uremic Patients Modulating miR-223 Expression in Plasma Extracellular Vesicles

Claudia Cavallari,*[,1] Sergio Dellepiane,[†,1] Valentina Fonsato,* Davide Medica,[†] Marita Marengo,[‡] Massimiliano Migliori,[§] Alessandro D. Quercia,[¶,‖] Adriana Pitino,* Marco Formica,[‡] Vincenzo Panichi,[§] Stefano Maffei,[†] Luigi Biancone,[†] Emanuele Gatti,[#] Ciro Tetta, Giovanni Camussi,[†] and Vincenzo Cantaluppi[¶,‖]**

Decreased inflammation and cardiovascular mortality are evident in patients with end-stage chronic kidney disease treated by online hemodiafiltration. Extracellular vesicles (EV) are mediators of cell-to-cell communication and contain different RNA types. This study investigated whether mixed online hemodiafiltration (mOL-HDF) beneficial effects associate with changes in the RNA content of plasma EV in chronic kidney disease patients. Thirty bicarbonate hemodialysis (BHD) patients were randomized 1:1 to continue BHD or switch to mOL-HDF. Concentration, size, and microRNA content of plasma EV were evaluated for 9 mo; we then studied EV effects on inflammation, angiogenesis, and apoptosis of endothelial cells (HUVEC) and on osteoblast mineralization of vascular smooth muscle cells (VSMC). mOL-HDF treatment reduced different inflammatory markers, including circulating CRP, IL-6, and NGAL. All hemodialysis patients showed higher plasma levels of endothelial-derived EV than healthy subjects, with no significant differences between BHD and mOL-HDF. However, BHD-derived EV had an increased expression of the proatherogenic miR-223 with respect to healthy subjects or mOL-HDF. Compared with EV from healthy subjects, those from hemodialysis patients reduced angiogenesis and increased HUVEC apoptosis and VSMC calcification; however, all these detrimental effects were reduced with mOL-HDF with respect to BHD. Cell transfection with miR-223 mimic or antagomiR proved the role of this microRNA in EV-induced HUVEC and VSMC dysfunction. The switch from BHD to mOL-HDF significantly reduced systemic inflammation and miR-223 expression in plasma EV, thus improving HUVEC angiogenesis and reducing VSMC calcification. ***The Journal of Immunology*****, 2019, 202: 000–000.**

Dialysis patients suffer from a high mortality, mostly related to vascular events (1, 2). Recently, several studies demonstrated an improvement of inflammatory parameters and of cardiovascular outcomes in patients with end-stage chronic kidney disease (CKD) treated by online hemodiafiltration (OL-HDF) (3–5). This cardioprotective effect may be ascribed to an enhanced clearance of middle molecules involved in CKD-associated inflammation, endothelial dysfunction, and vascular calcification (2, 6–8).

Increasing evidences indicate that plasma extracellular vesicles (EV) contribute to several physiological and pathological processes (9, 10). EV act as intercellular mediators by shuttling lipids, proteins, and predominantly extracellular RNAs (11, 12). Indeed, several biological activities of EV may be ascribed to the transfer of microRNAs (miRNAs), small noncoding RNAs able to regulate posttranscriptional expression of gene products (13). EV-carried miRNAs are protected from the activity of degrading enzymes, allowing their persistence in biological fluids and their delivery at distant sites. Recent studies have shown that plasma EV exert proinflammatory and prothrombotic properties and that EV may modulate endothelial function, suggesting a potential role of these microparticles in the pathogenesis of inflammatory disorders and atherosclerosis (14). Moreover, both EV and miRNAs circulating in the bloodstream reflect tissue damage and may be considered as

*2i3T SCARL, University of Turin, Turin 10126, Italy; [†]Nephrology, Dialysis and Kidney Transplantation Unit, Department of Medical Sciences, University of Turin, Turin 10126, Italy; [‡]Nephrology and Dialysis Unit, Local Health Service CN1, Cuneo 12100, Italy; [§]Nephrology and Dialysis Unit, Versilia Hospital, Camaiore, Lucca 55049, Italy; [¶]Nephrology and Kidney Transplantation Unit, Department of Translational Medicine, University of Piemonte Orientale, Novara 28100, Italy; [‖]Center for Translational Research on Autoimmune and Allergic Diseases, University of Eastern Piedmont, Novara 28100, Italy; [#]Department for Health Sciences and Biomedicine, Danube University, 3500 Krems, Austria; and **Unicyte SRL, Turin 10126, Italy

[1]C.C. and S.D. equally contributed.

ORCIDs: 0000-0003-1554-2999 (C.C.); 0000-0002-7133-4740 (S.D.); 0000-0002-6171-8919 (D.M.); 0000-0001-7149-4106 (M. Marengo); 0000-0001-8050-2120 (M. Migliori); 0000-0003-3772-6430 (A.P.); 0000-0001-7636-2356 (M.F.); 0000-0001-8621-0671 (S.M.); 0000-0002-4120-3555 (V.C.).

Received for publication May 31, 2018. Accepted for publication January 31, 2019.

This work was supported by a grant from Società Italiana di Nefrologia "Progetti Ricerca Scientifica" and Fondazione Cassa di Risparmio di Cuneo and Fondazione Cariplo and local university grants (University of Piemonte Orientale).

Address correspondence and reprint requests to Prof. Vincenzo Cantaluppi, S.C.D.U. Nefrologia e Trapianto Renale, Università degli Studi del Piemonte Orientale "Amedeo Avogadro," Azienda Ospedaliera Universitaria Maggiore della Carità, Via Solaroli 17, 28100 Novara, Italy. E-mail address: vincenzo.cantaluppi@med.uniupo.it

The online version of this article contains supplemental material.

Abbreviations used in this article: BHD, bicarbonate hemodialysis; CKD, chronic kidney disease; CRP, C-reactive protein; ERI, erythropoietin resistance index; EV, extracellular vesicle; IPA, ingenuity pathway analysis; miRNA, microRNA; mOL-HDF, mixed OL-HDF; NGAL, neutrophil gelatinase–associated lipocalin; OL-HDF, online hemodiafiltration; PQ, Protein Quest; PTH, parathyroid hormone; qRT-PCR, quantitative real-time PCR; RT, room temperature; VSMC, vascular smooth muscle cell.

biomarkers of disease activity (11, 15–18). Increased plasma levels of EV have been reported in hemodialysis patients in association with inflammatory parameters such as C-reactive protein (CRP) and IL-6 (19). However, it remains unclear whether the dialysis procedure itself may affect the release of EV, and the potential pathogenic role of EV-carried miRNAs in inflammation and vascular damage has not been fully elucidated. In this study, we hypothesized that circulating EV play a major role in dialysis-associated vascular dysfunction and that OL-HDF is beneficial to the vascular system also by modulating the circulating EV content of RNA.

The aims of the current study were (1) to isolate and characterize plasma EV derived from patients with end-stage CKD undergoing high-flux bicarbonate hemodialysis (BHD) before and after switching to mixed OL-HDF (mOL-HDF); (2) to analyze if different dialysis modalities modulate EV miRNAs potentially involved in inflammation, endothelial dysfunction, atherosclerosis, and vascular calcification.

Materials and Methods

Patients

Thirty patients undergoing regular high-flux BHD were enrolled in the study. Written informed consent was obtained. The study was conducted in accordance to Helsinki Declaration, approved by the Ethic Committee of the "Città della Salute e della Scienza di Torino" University Hospital (code 0030959, CEI/568), and registered in Clinicaltrials.gov (20). Inclusion criteria were as follows: age >18 y, hemodialysis from at least 6 mo (three times per week), blood flow rate (Qb) ≥ 250 ml/min using arteriovenous fistula or permanent central venous catheter, blood creatinine clearance <5 ml/min, urine output <500 ml/d. Exclusion criteria were as follows: neoplastic diseases, autoimmune diseases, solid organ or bone marrow transplantation. Enrolled patients were randomized to continue high-flux BHD (n = 15) or to switch to mOL-HDF (using FX 1000 CorDiax; Fresenius Medical Care, Bad Homburg, Germany; n = 15) for 9 mo (21). Immediately before the randomization (T0) and at 3 (T1), 6 (T2), and 9 (T3) mo after study start, the following parameters were evaluated: blood flow rate (ml/min), dialysate flow rate (ml/h), transmembrane pressure (mm Hg), convective volume exchange (l/session), net ultrafiltration (l/session), dialysis time (minutes), WBC count, hemoglobin, hematocrit, CRP, serum iron, transferrin saturation, ferritin, erythropoietin resistance index (ERI; Epo units/kg/wk/hemoglobin), β2-microglobulin, homocysteine, calcium, phosphate, parathyroid hormone (PTH), neutrophil gelatinase–associated lipocalin (NGAL). Dialysis adequacy was defined by Daugirdas' formula (eKt/V, where e indicates estimated; K, dialyzer clearance; t, time; V, urea volume of distribution), with a target value of 1.2; this is an accepted standard to estimate dialysis clearance of small molecules and is based on urea kinetics. In mOL-HDF sessions, a total convective volume >25 l was considered as appropriate.

Patients' plasma was collected at the beginning of the second dialysis session of the week at T0, T1, T2, and T3. Harvested samples were used to perform nanoparticle tracking analysis (22), Guava FACS, Western blot analysis, and cellular and molecular biology studies; plasma drawn from healthy subjects was used as negative control. Clinical and laboratory parameters of the enrolled patients were validated in a further cohort of hemodialysis patients treated by BHD (n = 50) or postdilution OL-HDF (n = 30), peritoneal dialysis patients (n = 10), and patients with stage IV CKD according to the Kidney Disease Outcomes Quality Initiative criteria (n = 20).

Table I. Demographic characteristics, comorbidities, dialysis age, and access type of enrolled patients

Patients' Characteristics	mOL-HDF	BHD	p
Gender (female)	23%	33%	0.2
Age	63.75 ± 11	65.5 ± 16.1	0.92
Hypertension	92%	83%	0.49
Diabetes	31%	25%	0.47
CV disease	31%	58%	0.16
Dialysis age (mo)	84 ± 75	82 ± 112	0.93
AVF	92%	83%	0.5

AVF, arteriovenous fistula; CV, cardiovascular.

Plasma collection and EV isolation

Patient and healthy control plasma was obtained by centrifuging peripheral blood in EDTA tubes at 6000 × g for 15 min at 20°C. To isolate EV, plasma samples were further centrifuged at 6000 × g for 20 min to remove remaining debris and then ultracentrifuged at 100,000 × g for 1 h at 4°C. EV were resuspended in 500 μl of RPMI 1640 with 1% DMSO and stored at −80°C.

Nanoparticle tracking analysis

EV preparations were diluted (1:1000) in sterile 0.9% saline solution and analyzed by NanoSight LM10 (Nanosight, Amesbury, U.K.) equipped with the Nanoparticle Analysis System & NTA 1.4 Analytical Software. The number of total EV for each patient was obtained by multiplying the value given by the instrument (microparticles/milliliter) for the dilution made for the analysis and for the number of ml in which EV were resuspended.

Guava FACS analysis

FACS analysis was performed on EV isolated from plasma by ultracentrifugation with GUAVA (GUAVA Easy-Cyte, EMD Millipore) for the following markers: exosomes (CD9, CD63, CD81, CD86), platelets (CD41, CD42b, CD62P), monocytes/macrophages (CD14, CD15), leukocytes (CD45), B cells (CD5, CD19, CD40), endothelial cells (CD31, CD105, CD144, CD146), T cells (CD3), and different markers involved in atherosclerosis and vascular senescence (tissue factor, C5b-9, CD40 ligand, ICOS, Fas ligand) (23, 24). Briefly, EV were labeled with fluorescence-conjugated Abs for 30 min at room temperature (RT). EV were washed twice in PBS with 0.5% BSA and resuspended in PBS 0.1% BSA. EV were analyzed using Guava Incyte Software version 3.1.1 (EMD Millipore). The acquired data files were analyzed first by adding an EV gate based on morphologic characteristics (forward scatter/side scatter) and subsequently by the use of the lineage-specific markers. FITC or PE mouse nonimmune isotypic IgG (Beckton Dickinson) were used as controls.

Electronic molecular network generation: Protein Quest

To detect relevant miRNAs, electronic literature screening was performed by the apposite web platform Protein Quest (PQ; Biodigital Valley, Aosta, Italy). PQ retrieves all biological and medical information from PubMed abstract and captions, free articles, United States patents, and clinical trials. Moreover, it classifies terminology by mesh biomedical dictionary and elaborates hierarchic networks displaying term relationships. By using an appropriate research string, we selected all available articles and abstracts regarding uremic vascular dysfunction or calcification; afterward, PQ recognized all described miRNAs and relative pathways.

Western blot analysis

EV proteins from four healthy individuals, four BHD patients, and four mOL-HDF patients were extracted using the radioimmunoprecipitation assay buffer (Sigma-Aldrich), supplemented with proteases and phosphatase inhibitors (Sigma-Aldrich), and then quantified using the Bradford assay

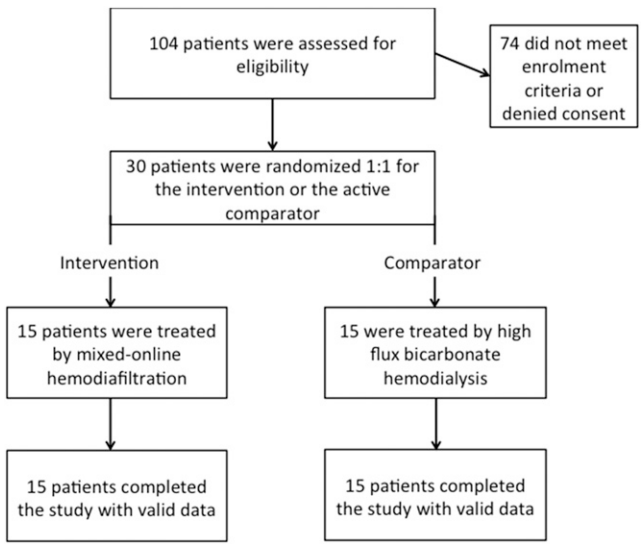

FIGURE 1. Study flowchart.

(BioRad). Briefly, 10 μg of EV proteins were subjected to SDS-PAGE, transferred onto nitrocellulose membranes, and underwent immunoblotting with Abs directed to anti-CD63 (1:200; Santa Cruz Biotechnology), anti-CD9 (1:2000; Abcam), and normalized to Actin (1:200; Santa Cruz Biotechnology). The same procedure was followed for HUVEC treated with EV from the different experimental groups using IGF1R Ab (1:200; Santa Cruz Biotechnology).

Cell culture

HUVEC were obtained by American Type Culture Collection (PCS-100-010-ATCC; Manassas, VA). HUVEC were plated with endothelial basal medium supplemented with 10% FCS (GE Healthcare, Boston, MA) and different endothelial growth factors as previously described (25). Human vascular smooth muscle cells (VSMC) were obtained by American Type Culture Collection (CRL-1999; ATCC) and grown in DMEM (GE Healthcare) with 10% of FCS. Both cell types represent an accepted standard to investigate vascular uremic dysfunction (26–29).

RNA extraction and quantitative real-time PCR

Total RNA from HUVEC, VSMC, or patients' EV was extracted using mirVana kit (Life Technologies), and analyzed by NanoDrop1000 spectrophotometer; samples of absorbance at 260/280 nm between 1.8 and 2.0 were adopted. We evaluated RUNX2 mRNA expression in VSMC by using High cDNA Reverse Transcription Kit and the Power SYBR Green PCR Master Mix on StepOnePlus Real Time System (Applied Biosystems). We used the web platform PQ (Biodigital Valley) to electronically screen the literature and to identify miRNA associated with uremic vascular dysfunction. Identified miRNA were detected in patients' EV using miScript Reverse Transcription Kit and miScript SYBR Green PCR Kit (Qiagen): 1 ml of blood was used for each quantification experiment. Primers of the selected miRNA (hsa-miR-17-5p, -92-a, -223, -423-5p, -451a), RUNX2, and housekeeping transcripts (actin-β and RNU48) are displayed in Supplemental Table I. Change in RNA expression was calculated using the $2^{-\Delta\Delta Ct}$ method. The miR-223 content was also analyzed in HUVEC or VSMC after transfection with specific mimic or antagomiR.

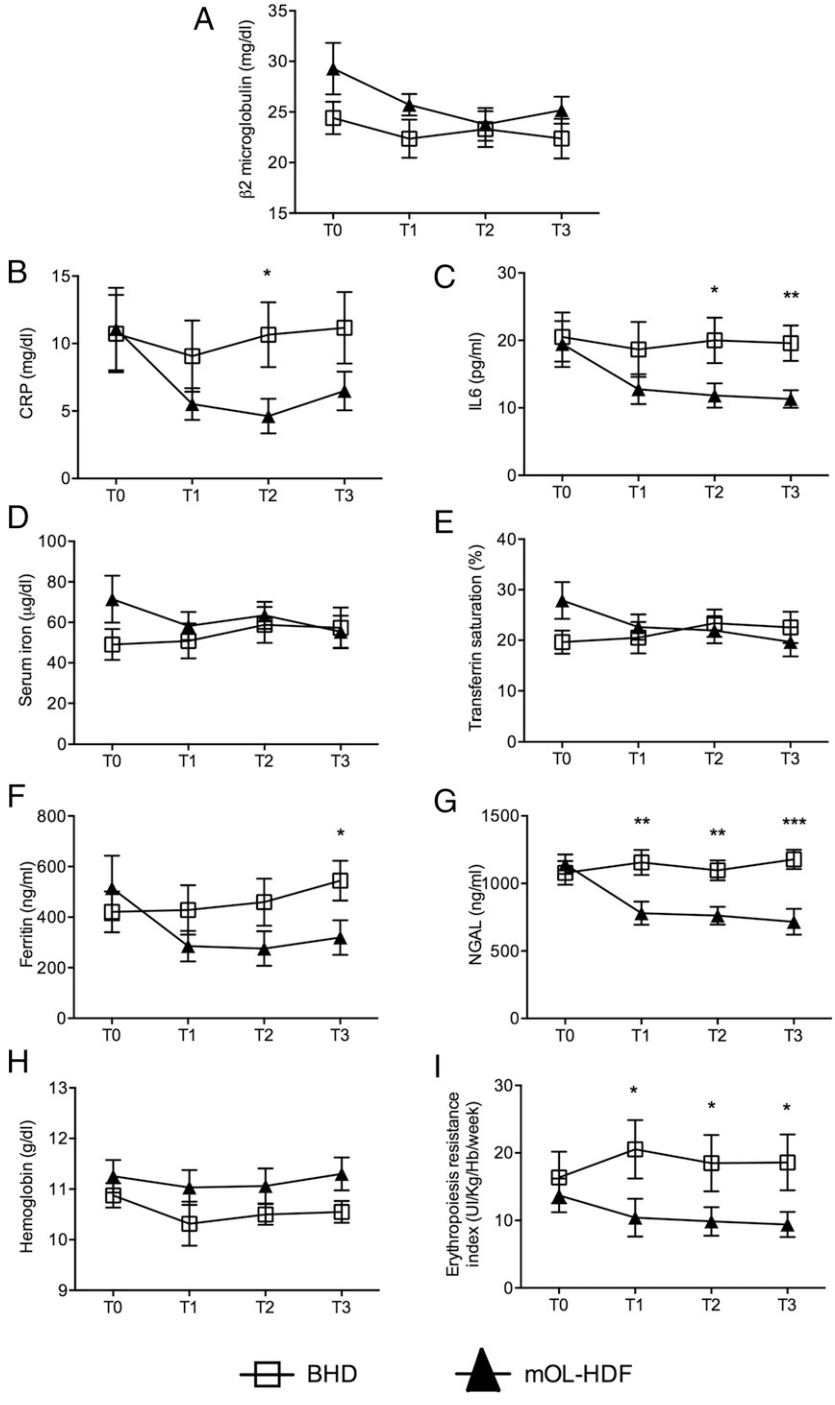

FIGURE 2. Clinical and intradialytic parameters: trend lines demonstrate the values of (**A**) β2-microglobulin, (**B**) CRP, (**C**) IL-6, (**D**) serum iron, (**E**) transferrin saturation, (**F**) ferritin, (**G**) NGAL, (**H**) hemoglobin, and (**I**) ERI across the study time points. $*p < 0.05$, $**p < 0.001$, $***p < 0.0001$ versus T0. T0, study start; T1, 3 mo after treatment start; T2, 6 mo after treatment start; T3, 9 mo after treatment start.

Table II. Patients'clinical variables at all considered time points

	T0		T1		T2		T3		p (ANOVA or χ^2)		
	mOL-HDF[a]	BHD	mOL-HDF	BHD	mOL-HDF	BHD	mOL-HDF	BHD	Within mOL-HDF	Within BHD	All
nPCR	1.12 ± 0.14	1.08 ± 0.12	1.16 ± 0.2	1.1 ± 0.15	1.18 ± 0.2	1.2 ± 0.12	1.15 ± 0.1	1.1 ± 0.18	0.92	0.89	0.88
Serum phosphate (mmol/l)	1.44 ± 0.6	1.42 ± 0.2	1.48 ± 0.3	1.41 ± 0.2	1.42 ± 0.3	1.38 ± 0.2	1.41 ± 0.4	1.44 ± 0.2	0.97	0.95	0.99
Serum calcium (mmol/l)	2.38 ± 0.2	2.36 ± 0.3	2.36 ± 0.2	2.37 ± 0.2	2.40 ± 0.3	2.33 ± 0.4	2.39 ± 0.3	2.38 ± 0.2	0.82	0.79	0.74
Serum PTH (pg/ml)	289 ± 205	234 ± 156	229 ± 167	267 ± 172	248 ± 164	221 ± 188	230 ± 127	256 ± 201	0.43	0.36	0.28
Number of HT drugs	1.6 ± 1.2	1.42 ± 1.1	1.5 ± 1.1	1.42 ± 1.1	1.6 ± 1.2	1.5 ± 1.2	1.6 ± 1.2	1.42 ± 1.1	0.97	0.94	0.88
i.v. iron (mg/wk)	37 ± 56	35 ± 22	39 ± 51	31 ± 24	42 ± 56	36 ± 24	50 ± 39	41 ± 21	0.82	0.76	0.88
Statin use	15%	33%	38%	33%	46%	33%	46%	33%	0.31	1	0.41
RAAS blocker	23%	15%	31%	15%	31%	25%	31%	25%	0.82	0.84	0.76
Vitamin D use	100%	100%	100%	92%	100%	92%	100%	92%	1	0.92	0.88
Pre-HD AP ≤ 140/90	69%	75%	69%	66%	84%	75%	84%	66%	0.76	0.65	0.82

[a]At T0, mOL-HDF group was still treated by BHD.
Statistical analysis was performed by one-way ANOVA or χ^2 test when appropriate. $p < 0.05$ was considered statistically significant.
AP, arterial pressure; HD, hemodialysis; HT, hypotensive; nPCR, normalized protein catabolic rate; RAAS, renin-angiotensin-aldosterone system.

Table III. Intradialytic variables at all considered time points

	T0		T1		T2		T3		p (ANOVA or χ^2)		
	mOL-HDF[a]	BHD	mOL-HDF	BHD	mOL-HDF	BHD	mOL-HDF	BHD	Within mOL-HDF	Within BHD	All
Dialyzer surface (m^2)	2 ± 0.15	2.0 ± 0.2	2 ± 0.15	2.0 ± 0.2	2 ± 0.15	2.0 ± 0.2	2 ± 0.15	2.0 ± 0.2	1	1	0.92
Heparin start dose (IU)	1250 ± 210	1458 ± 486	1250 ± 210	1458 ± 486	1250 ± 210	1458 ± 486	1250 ± 210	1458 ± 486	1	1	0.31
Heparin maintenance dose (IU/h)	307 ± 166	333 ± 144	307 ± 166	312 ± 136	307 ± 166	312 ± 136	307 ± 166	333 ± 144	1	0.91	0.68
HD duration (min)	237 ± 8	240 ± 0	237 ± 8	240 ± 0	237 ± 8	240 ± 0	237 ± 8	240 ± 0	1	1	0.63
Qb (ml/min)	317 ± 15	315 ± 18	320 ± 13	322 ± 21	318 ± 14	313 ± 16	319 ± 15	324 ± 26	0.96	0.76	0.65
Qd (ml/min)	500 ± 0	500 ± 0	468 ± 66	500 ± 0	459 ± 67	500 ± 0	466 ± 71	500 ± 0	0.88	1	0.08
Transmembrane pressure (mm Hg)	114 ± 13	115 ± 18	268 ± 12	118 ± 12	265 ± 11	112 ± 10	265 ± 12	108 ± 8	0.99	0.56	<0.01
Convective volume (l)	N/A	N/A	35.1 ± 4.6	N/A	33.8 ± 4	N/A	34.5 ± 4.2	N/A	0.92	N/A	N/A
Net ultrafiltration (l)	2.88 ± 0.52	2.75 ± 0.47	2.76 ± 0.54	2.92 ± 0.58	2.85 ± 0.49	3 ± 0.64	2.84 ± 0.43	2.76 ± 0.5	0.78	0.47	0.65
eKt/V	1.34 ± 0.23	1.38 ± 0.24	1.48 ± 0.27	1.36 ± 0.24	1.68 ± 0.34	1.37 ± 0.26	1.48 ± 0.28	1.38 ± 0.22	0.04	0.98	0.03

[a]At T0, mOL-HDF group was still treated by BHD.
Statistical analysis was performed by one-way ANOVA or χ^2 test when appropriate. $p < 0.05$ was considered statistically significant.
HD, hemodialysis; Qb, blood flow; Qd, dialysis solution flow.

In vitro angiogenesis of endothelial cells

HUVEC were seeded into Matrigel-coated wells (1.5×10^4 cells/well) in endothelial basal medium with or without patients' EV. Vascular endothelial growth factor (10 ng/ml) and uremic toxins (ADMA 10 μg/ml, p-cresyl sulfate 1 μg/ml, and indoxyl sulfate 10 μg/ml) were used as positive or negative control, respectively. Experimental results were recorded with a Nikon inverted microscope after 24 h of incubation with different stimuli at 37˚C. Image analysis of capillary-like structures was performed using the ImageJ Analysis System. Results were given as average number of capillary-like structures/field ±1 SD (magnification ×10). In all the assays, cells were stimulated with EV isolated from 1 ml of patients' blood for each 10 ml of medium.

In vitro apoptosis of endothelial cells

HUVEC were cultured in 96 flat-bottom microtiter plates at a concentration of 2×10^4 cells/well. Cells were examined after 24 h of stimulation at 37˚C. Vascular endothelial growth factor and uremic toxins were used as negative or positive control, respectively. HUVEC were resuspended in 100 μl of RPMI 1% BSA, then mixed with 100 μl of Muse Annexin V and Dead Cell reagent, incubated for 20 min at RT, and analyzed by the Muse Cell Analyzer (EMD Millipore). In all the assays, cells were stimulated with EV isolated from 1 ml of patients' blood for each 10 ml of medium.

Osteoblastic differentiation of VSMC

VSMC were fixed in 50% ethanol at RT for 10 min, stained with 10 mg/ml alizarin red for 5 min, and washed twice in PBS. Retained dye was extracted with a solution of 20% methanol and 10% acetic acid; the absorbance at 450 nm was then measured (30).

Cell transfection

Transfection of miR-223 mimic (10 nM) or miR-223 inhibitor (100 nM) was performed on HUVEC or VSMC using HiPerfect Transfection method (Qiagen, Valencia, CA). The expression of miR-223 was evaluated by quantitative real-time PCR (qRT-PCR). Data were expressed as log of relative quantification, normalized to RNU-48.

Direct transfection of miR-223 inhibitor was performed coincubating miR-223 inhibitor and BHD-EV followed by HUVEC or VSMC treatment. Angiogenesis and calcification effects were evaluated as reported.

Statistical analysis

Unless otherwise indicated, all data are shown as mean ± SEM. Statistical analysis was performed using the unpaired Student *t* test, ANOVA, or Kruskal–Wallis test when appropriate. A two-sided value of $p = 0.05$ was considered significant.

Results

Clinical and dialysis parameters

The main clinical characteristics of enrolled patients are described in Table I: no significant differences were found between BHD and mOL-HDF patients in terms of gender, age, prevalence of hypertension, diabetes and cardiovascular diseases, dialysis vintage, and vascular access type. All enrolled patients completed the study with valid data (Fig. 1).

As expected from previously published randomized clinical trials, the switch from BHD to mOL-HDF was associated with an improvement of inflammatory parameters: indeed, we observed a significant decrease in plasma CRP ($p = 0.05$), ferritin ($p = 0.04$), IL-6 ($p < 0.001$), and NGAL ($p = 0.007$) in mOL-HDF patients between T0 and T1 (Fig. 2). Consistently, the modulation of the inflammatory state was confirmed by the improvement of ERI ($p = 0.05$). A decrease of β2-microglobulin not reaching statistical significance ($p = 0.12$) was also observed. No significant differences were found in hemoglobin levels, transferrin saturation, and homocysteine (data not shown). By contrast, patients maintained

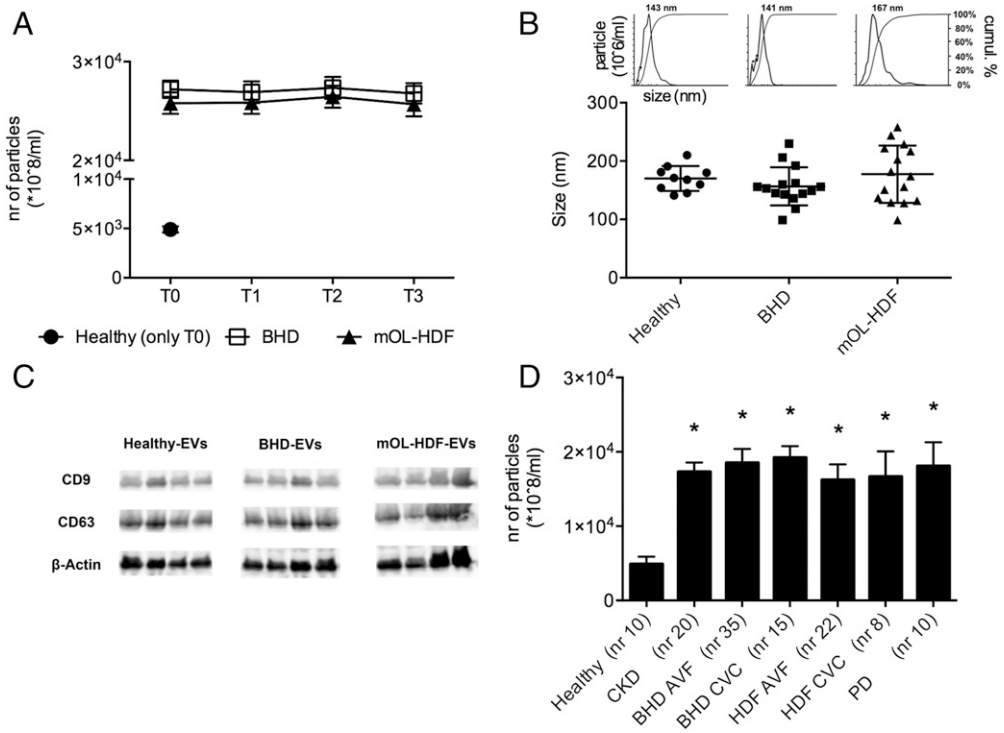

FIGURE 3. Nanosight and Western blot analysis of plasma EV. (**A**) Plasma EV concentration at the different study time points in patients randomized to BHD ($n = 15$) or mOL-HDF ($n = 15$) and in a group of healthy subjects (only T0). (**B**) Representative Nanosight Tracking Analysis plots and medium EV size for each healthy subject, BHD patient, and mOL-HDF patient enrolled. (**C**) Representative Western Blot analysis of CD9, CD63, and β-actin protein content in healthy, BHD-, and mOL-HDF–EV. (**D**) EV quantification in the control cohort of healthy subjects ($n = 10$), stage IV CKD ($n = 20$), peritoneal dialysis (PD) ($n = 10$), BHD hemodialysis ($n = 50$), or postdilution OL-HDF patients ($n = 30$). Hemodialysis patients were subdivided according to vascular access type (arteriovenous fistula [AVF], $n = 57$; central venous catheter [CVC], $n = 23$). Statistical analysis was performed by ANOVA with Newman–Keuls multicomparison test. *$p < 0.05$ versus healthy. (m)OL-HDF, (mixed) OL-HDF; T0, study start; T1, 3 mo after treatment start; T2, 6 mo after treatment start; T3, 9 mo after treatment start.

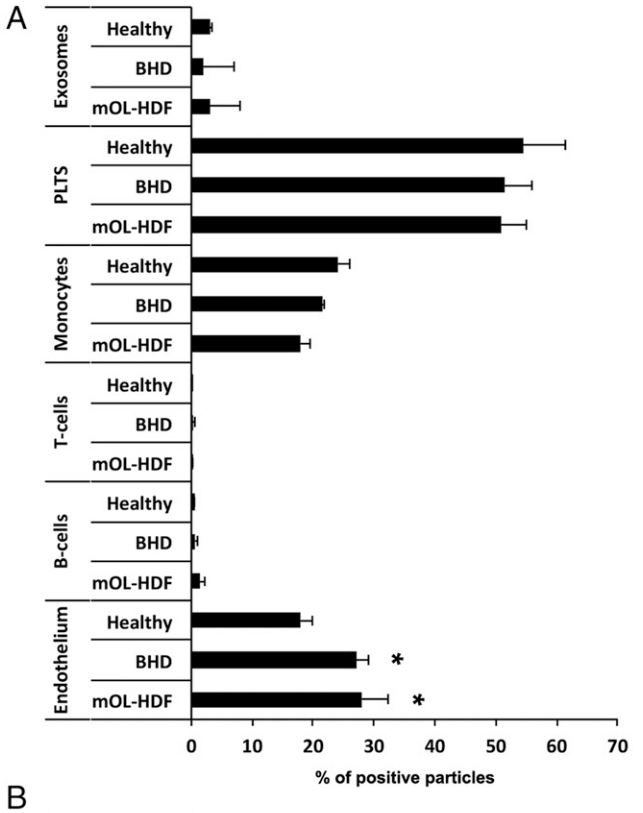

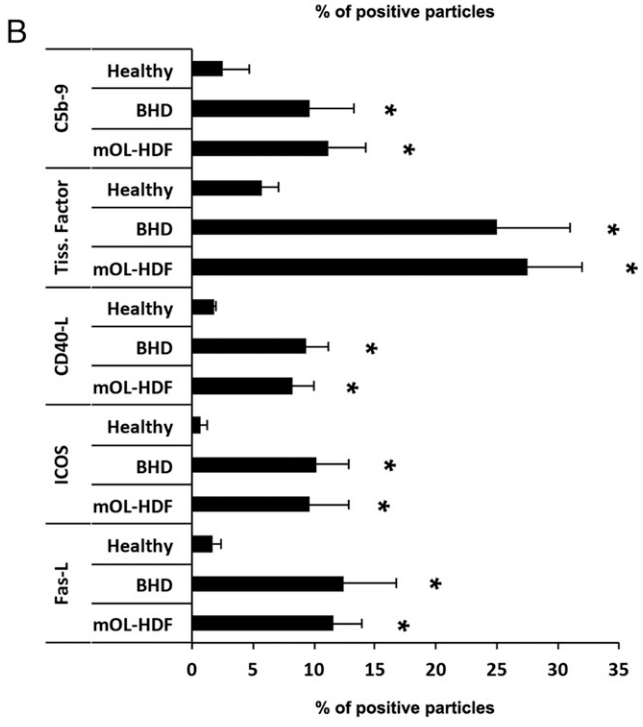

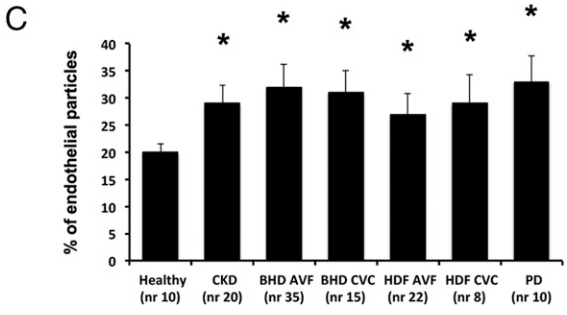

in BHD did not show significant changes in any of the measured parameters. To exclude possible confounding factors, we also analyzed different clinical/therapeutic variables including nutritional and hemodynamic status; serum levels of calcium, phosphate, and PTH; i.v. use of iron; treatment with statins, renin-angiotensin-aldosterone system antagonists, or vitamin D (reported in detail in Table II); and intradialytic variables (filter surface, heparin dose, treatment duration, blood and dialysis solution flow, transmembrane pressure, dialysis efficiency, and convective volumes reported in detail in Table III) at all the time points considered. As expected, mOL-HDF treatment was associated with a higher transmembrane pressure and with an improved eKt/V. All the other variables were comparable in the two groups at all considered time points.

Analysis of plasma EV

At study admission (T0), dialysis patients showed higher plasma EV concentration than healthy subjects, and EV concentration did not change through the study time points within the groups (Fig. 3A). EV size distribution showed similar results among the different groups with a mean size of 170 nm (Fig. 3B). Moreover, EV expressed typical exosomal markers such as CD9 and CD63 (Fig. 3C). Results concerning EV concentration were confirmed in a further cohort of 80 patients undergoing chronic hemodialysis (n = 50 in BHD and n = 30 in postdilution OL-HDF), 10 patients in peritoneal dialysis, and 20 patients with stage IV CKD according to Kidney Disease Outcomes Quality Initiative guidelines. Hemodialysis patients were further classified according to vascular access type (arteriovenous fistula versus central venous catheter): all groups were matched for age and gender. CKD stage IV and all peritoneal and hemodialysis patients showed a 5-fold increase of circulating plasma EV in comparison with healthy subjects (Fig. 3D).

Guava FACS analysis of EV from dialysis patients at T0 revealed that the majority of circulating microparticles derived from platelets, monocytes/macrophages, and endothelial cells; only endothelial EV were upregulated in comparison with healthy subjects (Fig. 4A, Supplemental Fig. 1). In both groups, no changes in terms of cell-specific markers were found across the study time points (data not shown). Of interest, plasma EV of enrolled patients expressed surface markers involved in inflammation, atherosclerosis, and complement and coagulation activation [CD40 ligand, ICOS, Fas ligand, C5b-9, tissue factor (Fig. 4B, Supplemental Fig. 2)]. Consistently, an increased percentage of endothelial-derived particles was observed in all the different control groups [stage IV CKD, peritoneal dialysis, or hemodialysis independently from vascular access type or dialysis modality (Fig. 4C)].

FIGURE 4. Guava FACS analysis of plasma EV. (**A**) Histograms showing the positivity rate (%) for exosome, platelet, monocyte/macrophage, T cell, B cell, and endothelial cell markers (see *Materials and Methods*) in EV derived from healthy subjects, BHD, or mOL-HDF patients at study start. (**B**) Histograms showing the positivity rate (%) for marker of uremia-related atherosclerosis and inflammation in EV derived from healthy subjects, BHD, or mOL-HDF patients at study start. (**C**) Quantification of endothelial-derived EV in the control cohort of healthy subjects (n = 10), stage IV CKD (n = 20), peritoneal dialysis (PD) (n = 10), BHD hemodialysis (n = 50), or postdilution OL-HDF patients (n = 30). Hemodialysis patients were subdivided according to vascular access type (arteriovenous fistula [AVF], n = 57; central venous catheter [CVC], n = 23). Statistical analysis was performed by ANOVA with Newman–Keuls multicomparison test. *$p < 0.05$ versus healthy. (m)OL-HDF, (mixed) OL-HDF; T0, study start; T1, 3 mo after treatment start; T2, 6 mo after treatment start; T3, 9 mo after treatment start.

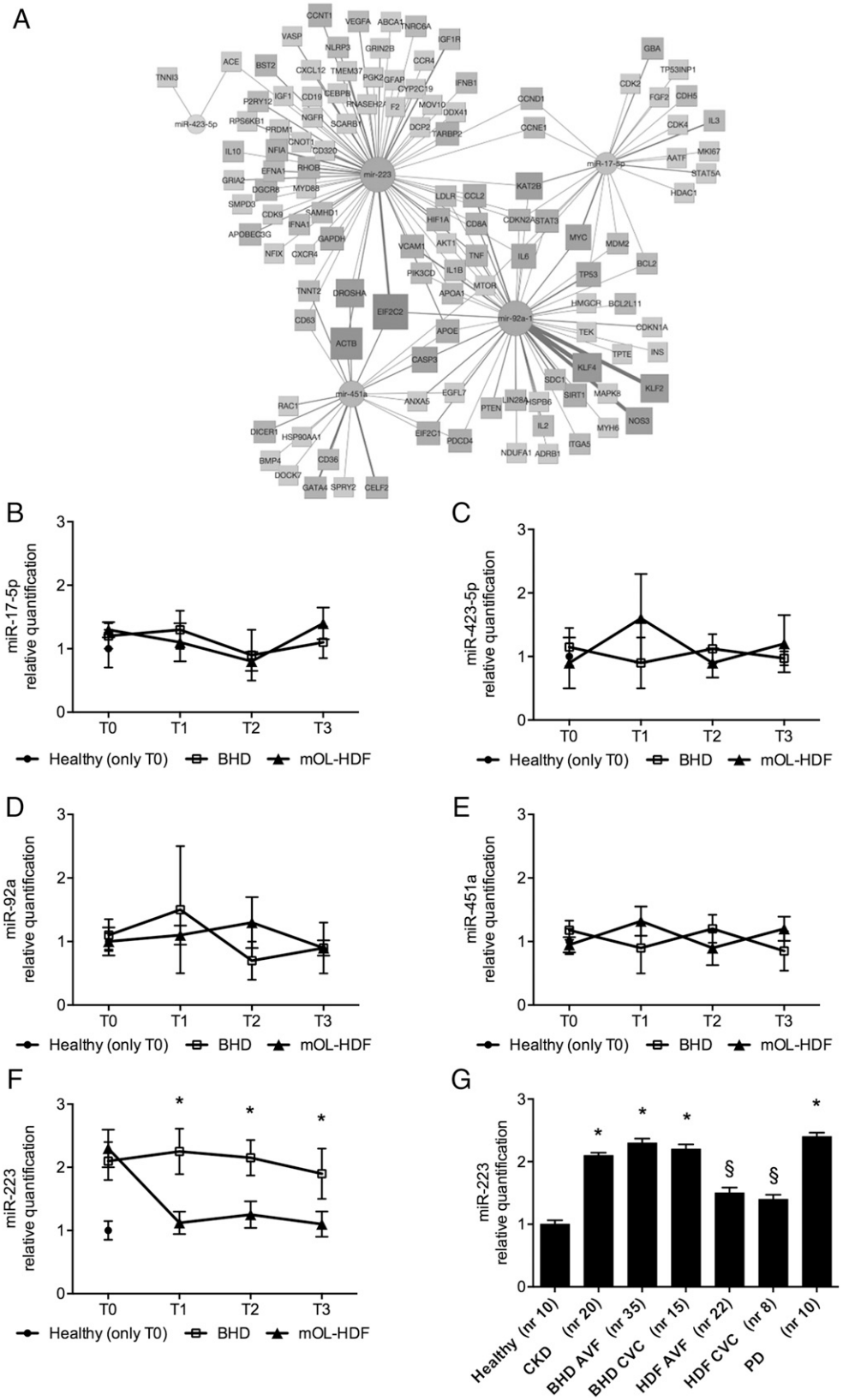

FIGURE 5. Analysis of miRNA content in plasma EV of hemodialysis patients. (**A**) PQ web-based analysis identified five different miRNAs (miR-17a-5p, miR-92a, miR-223, miR-423-5p, and miR-451) involved in endothelial dysfunction and vascular calcification. Squares represent miRNAs, whereas circles represent proteins. Node dimension correlates with literature frequency of displayed molecules; line thickness represents the number of literature co-occurrence between elements. (**B**–**F**) Relative quantification by RT-PCR for EV expression of the five identified miRNAs in healthy controls, BHD patients, and mOL-HDF patients at the different study time points. (**G**) qRT-PCR for miR-223 in the control cohort of healthy subjects (n = 10), stage IV CKD (n = 20), peritoneal dialysis (PD) (n = 10), BHD hemodialysis (n = 50), or postdilution OL-HDF patients (n = 30). Hemodialysis patients were subdivided according to vascular access type (arteriovenous fistula [AVF], n = 57; central venous catheter [CVC], n = 23). Statistical analysis was performed by ANOVA with Newman–Keuls multicomparison test. *$p < 0.05$ versus healthy, $^{\S}p < 0.05$ versus BHD. (m)OL-HDF, (mixed) OL-HDF; T0, study start; T1, 3 mo after treatment start; T2, 6 mo after treatment start; T3, 9 mo after treatment start.

Characterization of miRNA content of plasma EV

By PQ analysis (Fig. 5A), five different miRNAs involved in endothelial dysfunction and vascular calcification were identified (miR-17-5p, miR-92a, miR-223, miR-423-5p, and miR-451). The expression of these miRNAs was analyzed through all the study time points by qRT-PCR. The expression of miR-17-5p, miR-92a, miR-423-5p, and miR-451 was not significantly different among healthy control, BHD-, and mOL-HDF–derived EV (Fig. 5B–E). By contrast, EV derived from dialysis patients showed an increased expression of miR-223 at T0 if compared with healthy controls; subsequently, mOL-HDF patients displayed a significant decline of EV miR-223 expression that was not observed in BHD patients and was maintained at all the time points considered (Fig. 5F). Patients from the control cohort treated by postdilution OL-HDF had reduced levels of EV-carried miR-223 if compared with stage IV CKD patients, peritoneal dialysis patients, and BHD-treated patients (Fig. 5G).

Role of plasma EV-carried miR-223 in endothelial dysfunction

Because we identified a decreased expression of miR-223 in EV derived from mOL-HDF patients with respect to BHD patients, we performed in vitro experiments to evaluate the specific role of this miRNA in endothelial dysfunction. With respect to EV collected from healthy subjects, BHD-derived EV reduced the formation of capillary-like structures by HUVEC (Fig. 6A). This antiangiogenic effect was similar to what was observed in presence of known uremic toxins (ADMA, p-cresyl sulfate, and indoxyl sulfate). HUVEC angiogenesis was significantly higher with mOL-HDF–derived EV than with BHD-EV, even if not reaching the level observed with healthy EV. Similar results were also observed in experiments aimed to evaluate HUVEC apoptosis (Fig. 6B).

To investigate whether miR-223 was involved in the antiangiogenic and proapoptotic activities of plasma EV, we evaluated the effect of specific mimic and antagomiR transfection, respectively. HUVEC transfected with mimic miR-223 showed a significant reduction of in vitro angiogenic response when challenged with healthy plasma EV, as well as with EV derived from dialysis patients. Conversely, transfection of HUVEC with miR-223–antagomiR significantly restored the angiogenic potential of plasma EV, particularly in presence of BHD-derived EV (Fig. 6C). The levels of expression of miR-223 in all experimental conditions were verified by qRT-PCR (Supplemental Fig. 3). Transfection of AntagomiR-223 was also used to inhibit miR-223 directly in BHD-EV. As shown in Fig. 6D, transfected BHD-EV significantly restored proangiogenic properties on target cells, indicating that EV can deliver miR-223.

Role of plasma EV-carried miR-223 in VSMC calcification

We also investigated the role of EV-carried miR-223 in osteoblastic differentiation of VSMC. As shown by red alizarin staining and RUNX2 expression, EV derived from BHD patients induced an increase of VSMC calcification (Fig. 7A–C). By contrast, EV derived from mOL-HDF patients did not increase VSMC osteoblastic differentiation when compared with healthy subject particles. VSMC transfected with mimic miR-223 showed an increase of osteoblastic differentiation when incubated with healthy plasma EV, as well as with plasma EV derived from BHD and mOL-HDF patients. Conversely, transfection of VSMC with miR-223–antagomiR significantly reduced the calcification potential of plasma EV, particularly in presence of BHD-derived EV (Fig. 7D). Moreover, direct transfection of miR-223 inhibitor in BHD-EV led to a significant decrease of calcification potential induced by BHD-EV (Fig. 7E).

Evaluation of miR-223 target genes

To investigate the role of miR-223 in endothelial dysfunction, we analyzed the potential target genes in HUVEC. The network predicted by ingenuity pathway analysis (IPA) for miR-223 showed IGF1R as the most likely target (Fig. 8A). We then evaluated

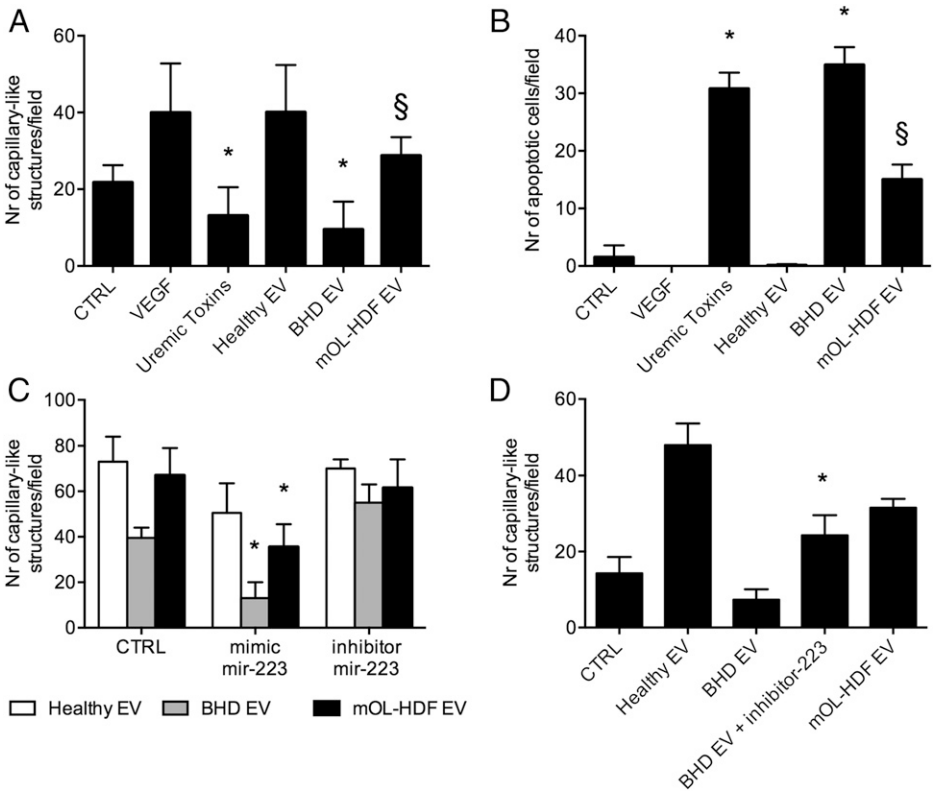

FIGURE 6. Effect of plasma EV on in vitro endothelial angiogenesis and apoptosis. (**A**) Histogram showing the quantitative analysis of the in vitro HUVEC angiogenesis assay after different stimuli. $*p < 0.05$ versus CTRL, $^{§}p < 0.05$ versus BHD-EV. (**B**) Histogram showing the quantitative analysis of the in vitro TUNEL apoptosis assay on HUVEC subjected to different stimuli. $*p < 0.05$ versus CTRL, $^{§}p < 0.05$ versus BHD-EV. (**C**) Quantitative analysis of angiogenesis assay in HUVEC transfected with miR-223 mimic or inhibitor and stimulated with patients' EV. $*p < 0.05$ versus the corresponding CTRL column. (**D**) Quantitative analysis of HUVEC angiogenesis assay after stimulation with patients' EV transfected or not with miR-223 inhibitor. Uremic Toxins: asymmetric dimethylarginine 10 μg/ml + p-cresyl sulfate 1 μg/ml and indoxyl sulfate 10 μg/ml. $*p < 0.05$ versus BHD EV. CTRL, control group; VEGF, vascular endothelial growth factor.

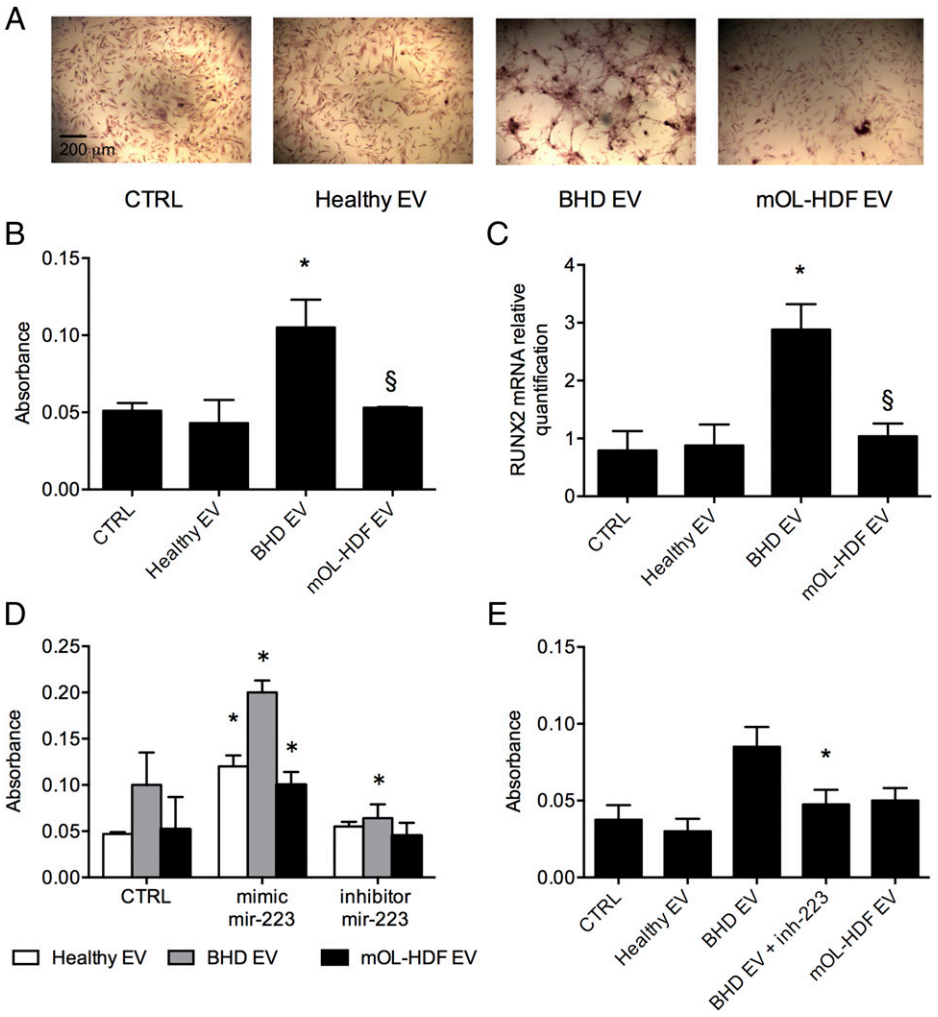

FIGURE 7. Role of plasma EV-carried miR-223 in osteoblastic differentiation of VSMC. (**A**) Representative images and (**B**) relative quantification of red alizarin staining of VSMC incubated with EV derived from healthy subjects, BHD, or mOL-HDF patients. $*p < 0.05$ versus healthy EV, $^{\S}p < 0.05$ versus BHD EV. (**C**) qRT-PCR for RUNX2 mRNA expression in VSMC incubated with EV derived from healthy subjects, BHD, or mOL-HDF patients. $*p < 0.05$ versus healthy EV, $^{\S}p < 0.05$ versus BHD EV. (**D**) Quantitative analysis of red alizarin staining in VSMC transfected with miR-223 mimic or inhibitor and stimulated with patients' EV. $*p < 0.05$ versus the corresponding CTRL column. (**E**) Quantitative analysis of VSMC staining after stimulation with patients EV transfected or not with miR-223 inhibitor. $*p < 0.05$ versus BHD EV. CTRL, control group.

whether miR-223 delivered by BHD-EV may modulate IGF1R expression in HUVEC. Western blot analysis demonstrated that treatment of HUVEC with BHD-EV significantly reduced IGF1R expression when compared with cells stimulated with BHD-EV + inhibitor–miR-223 (Fig. 8B, 8C). A similar decrease was also observed when HUVEC were incubated with mimic-223, thus confirming miR-223 action on IGF1R. Although a previous study suggested β1-integrin as a further miR-223 target, we did not find any expression change of this protein in HUVEC (data not shown) (31).

Discussion

In this study, we evaluated the quantitative and qualitative changes of plasma EV in a population of patients with end-stage CKD after switching from high-flux BHD to mOL-HDF. We found that mOL-HDF was associated with a modulation of EV miR-223; additionally, our in vitro data suggested a role of miR-223 in CKD-related endothelial dysfunction and vascular calcification. As already reported in previous studies (2, 5–7), the use of a mixed convective-diffusive hemodepuration led to a significant decrease of inflammatory parameters such as CRP, ferritin, IL-6, NGAL, and ERI. NGAL is a 25-KDa protein belonging to the calycin family that has been proposed as marker of inflammation and reduced iron bioavailability in hemodialysis patients (32, 33).

Systemic inflammation is a hallmark of CKD and plays a key role in the development and progression of cardiovascular diseases. HDF with high convection volumes is currently considered the most effective technique for achieving a better clearance of middle molecules in patients with end-stage CKD (5). Several studies have shown that HDF improves intradialytic hemodynamic stability and some CKD complications, such as inflammation, malnutrition, erythropoietin-resistant anemia, and dialysis-associated amyloidosis. Large observational studies (Dialysis Outcomes and Practice Patterns Study, Euclid, and Riscavid) and randomized control trials (Eshol) demonstrated improved overall and cardiovascular survival in patients treated with HDF versus BHD (7, 8, 34, 35). Based on these studies, higher convective volumes are probably responsible for an enhanced clearance of middle/large uremic toxins involved in the development of cardiovascular complications and anemia (36). Postdilution HDF is the most efficient infusion mode to maximize clearance of small and large solutes; nevertheless, this approach increases the frequency of technical problems due to hemoconcentration and high transmembrane pressure. The simultaneous use of pre- and postdilution offered by mOL-HDF may avoid the disadvantages of traditional infusion modes. Indeed, in mOL-HDF, pre- and postinfusion percentages are automatically regulated through transmembrane pressure and ultrafiltration feedback (37). Recent studies compared the clearance of small, medium-sized, and protein-bound molecules and the convective volume administered in standard postdilution OL-HDF versus mOL-HDF without finding any significant difference. Moreover, mOL-HDF allows achieving a satisfactory convective volume exchange, even in patients with suboptimal blood flow rates due to vascular access problem (21).

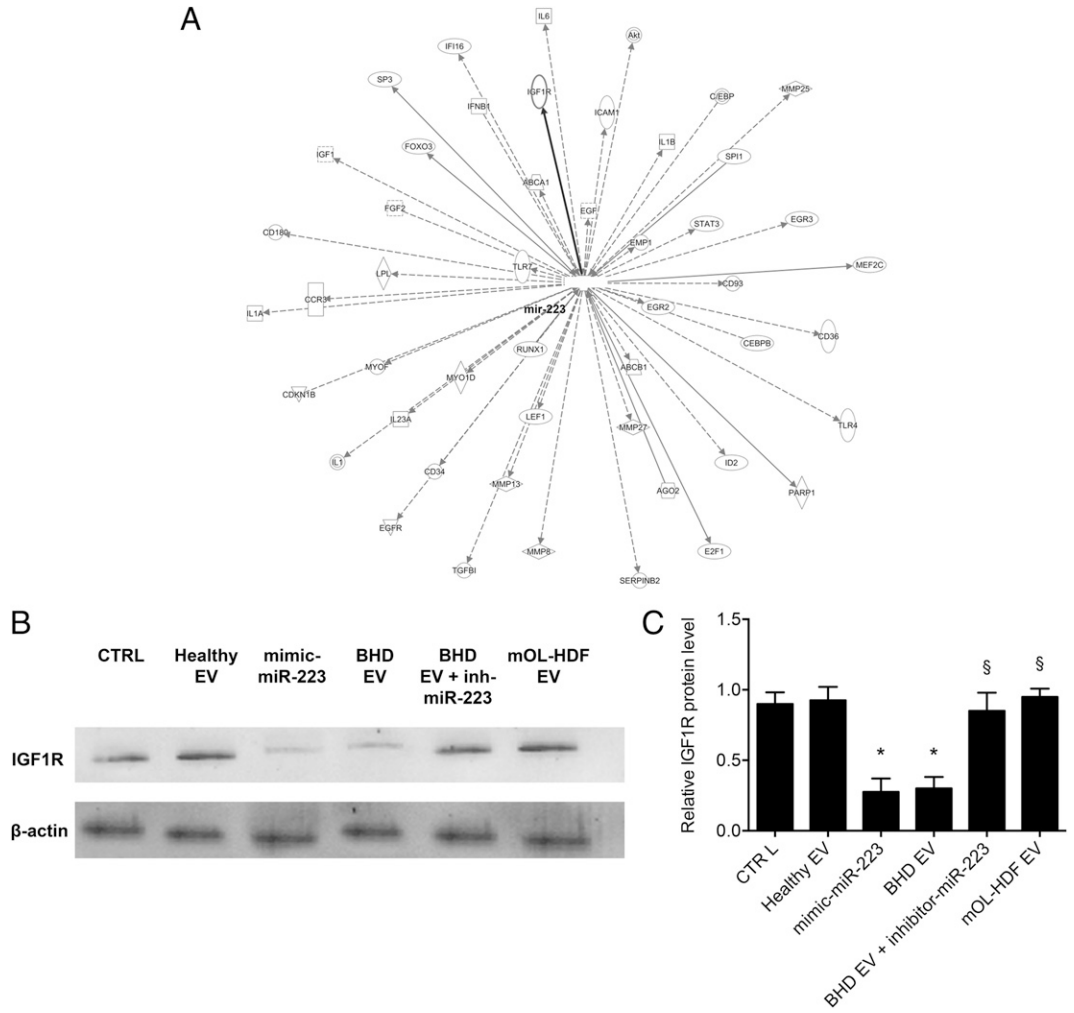

FIGURE 8. Analysis of miR-223 target genes: role of IGF1R. (**A**) IPA predicted target genes for miR-223. Arrowheads represent activating relationships, whereas solid or dotted edges indicate direct or indirect relationships, respectively. Relationship between miR-223 and IGF1R is highlighted. (**B**) Representative Western Blot analysis and (**C**) relative quantification of IGF1R protein expression in HUVEC after stimulation with healthy, BHD, or mOL-HDF patient EV or after transfection with miR-223 mimic, or after stimulation with BHD patient EV transfected with miR-223 inhibitor. $*p < 0.05$ versus healthy, $^{\S}p < 0.05$ mimic-223 versus BHD. CTRL, control group; IGF1R: insulin like growth factor 1 receptor.

The influence of uremia-related inflammation on circulating plasma EV has been poorly investigated. It is well established that EV represent an important vehicle of intercellular communication due to their ability in transporting molecules such as proteins, surface receptors, lipids, mRNA, and, particularly, miRNA (11, 38). A significant increase of plasma EV is associated with several inflammatory diseases characterized by endothelial dysfunction and vascular calcification (19). In the current study, we found that CKD patients treated by high-flux BHD or mOL-HDF presented higher levels of plasma EV when compared with healthy subjects matched for age and gender. Moreover, the analysis of surface Ags revealed the increase of EV expressing typical endothelial markers, suggesting the presence of ongoing microvascular damage. Furthermore, EV surface protein analysis revealed the presence of molecules involved in coagulation and complement cascades (tissue factor, C5b-9) and in the pathogenic mechanisms of inflammation and atherosclerosis: CD40 ligand, ICOS, and Fas ligand. These latter receptors are deeply involved in the destabilization of atherosclerotic plaques: ICOS/ICOS ligand activation has been recently shown to play a key role in the proatherogenic activation of the T follicular/B cell axis (39); similarly, both CD40 and CD40 ligand are largely expressed in atherosclerotic plaques and in vascular calcifications of uremic patients (23, 40). In addition, the blockade of CD40/CD40 ligand pathway led to a significant reduction of vascular damage in atherosclerosis-prone mice (41). Last, our research group previously demonstrated that soluble CD40 ligand levels are predictive of combined cardiovascular morbidity and mortality in dialysis patients (42). Based on these considerations, one could speculate that CD40 ligand, ICOS, and Fas ligand expressed by uremic EV may directly activate the counterreceptors expressed on endothelial cells and smooth muscle cells, leading to plaque destabilization. However, different studies showed that the biological activities of EV are mainly ascribed to the transfer of RNA to target cells (38, 43, 44). In the current study, although we did not detect any significant difference between the two dialysis modalities in terms of concentration, size, and surface Ags, we observed that EV isolated after switching to mOL-HDF presented a variation of miRNA content. Of interest, after the switch to mOL-HDF, we found a decreased expression of miR-223, which is potentially involved in endothelial dysfunction and vascular calcification (32, 45–50) and is considered a biomarker of atherosclerosis progression (46, 51). Indeed, miR-223 inhibits angiogenesis by targeting β1-integrin and by preventing insulin-like growth factor 1 signaling in endothelial cells (31); moreover, a recent study reported that miR-223 is also involved in osteoblast differentiation of VSMC (52).

The decrease of EV miR-223 found in mOL-HDF group was also observed in another cohort of hemodialysis patients regularly treated by postdilution OL-HDF: this reduction was independent from the vascular access type and not observed in peritoneal dialysis patients and BHD-treated patients. These findings suggest that high-volume HDF is responsible for modulation of proinflammatory and proatherogenic miRNA expression within plasma EV.

Furthermore, in our in vitro experiments, the increased expression of miR-223 in EV from BHD patients was associated with HUVEC angiogenesis inhibition, increased endothelial apoptosis, and enhanced VSMC calcification. Of note, all these detrimental effects were downregulated by mOL-HDF. Consistently, experiments based on miR-223 mimic or antagomiR confirmed the relevance of this transcript in the biological activity of BHD-derived EV. Finally, we found that EV-carried miR-223 may modulate different intracellular pathways involved in endothelial angiogenesis and apoptosis, including IGF1R, as suggested by IPA network analysis.

In conclusion, the results of the current study indicate that EV derived from hemodialysis patients express surface proteins and carry miRNAs involved in inflammation-related endothelial dysfunction and vascular calcification. Switching from BHD to mOL-HDF significantly decreased the expression of EV miR-223 but not of other miRNAs. The in vitro experiments indicated that the reduced expression of miR-223 justifies, at least partially, the decreased detrimental effect of plasma EV from mOL-HDF patients. These results may contribute to explaining the protective effects on endothelial dysfunction and vascular calcification observed in OL-HDF clinical studies.

Disclosures

The authors have no financial conflicts of interest.

References

1. Gai, M., I. Merlo, S. Dellepiane, V. Cantaluppi, G. Leonardi, F. Fop, C. Guarena, G. Grassi, and L. Biancone. 2014. Glycemic pattern in diabetic patients on hemodialysis: continuous glucose monitoring (CGM) analysis. *Blood Purif.* 38: 68–73.
2. Maduell, F., F. Moreso, M. Pons, R. Ramos, J. Mora-Macià, J. Carreras, J. Soler, F. Torres, J. M. Campistol, and A. Martinez-Castelao, ESHOL Study Group. 2013. High-efficiency postdilution online hemodiafiltration reduces all-cause mortality in hemodialysis patients. *J. Am. Soc. Nephrol.* 24: 487–497.
3. den Hoedt, C. H., M. L. Bots, M. P. Grooteman, N. C. van der Weerd, A. H. Mazairac, E. L. Penne, R. Levesque, P. M. ter Wee, M. J. Nubé, P. J. Blankestijn, and M. A. van den Dorpel, CONTRAST Investigators. 2014. Online hemodiafiltration reduces systemic inflammation compared to low-flux hemodialysis. *Kidney Int.* 86: 423–432.
4. Grooteman, M. P., M. A. van den Dorpel, M. L. Bots, E. L. Penne, N. C. van der Weerd, A. H. Mazairac, C. H. den Hoedt, I. van der Tweel, R. Lévesque, M. J. Nubé, et al; CONTRAST Investigators. 2012. Effect of online hemodiafiltration on all-cause mortality and cardiovascular outcomes. *J. Am. Soc. Nephrol.* 23: 1087–1096.
5. Panichi, V., G. M. Rizza, S. Paoletti, R. Bigazzi, M. Aloisi, G. Barsotti, P. Rindi, G. Donati, A. Antonelli, E. Panicucci, et al; RISCAVID Study Group. 2008. Chronic inflammation and mortality in haemodialysis: effect of different renal replacement therapies. Results from the RISCAVID study. *Nephrol. Dial. Transplant.* 23: 2337–2343.
6. Ok, E., G. Asci, H. Toz, E. S. Ok, F. Kircelli, M. Yilmaz, E. Hur, M. S. Demirci, C. Demirci, S. Duman, et al; Turkish Online Haemodiafiltration Study. 2013. Mortality and cardiovascular events in online haemodiafiltration (OL-HDF) compared with high-flux dialysis: results from the Turkish OL-HDF study. *Nephrol. Dial. Transplant.* 28: 192–202.
7. Pérez-García, R. 2014. On-line haemodiafiltration after the ESHOL study. *Nefrologia* 34: 139–144.
8. Panichi, V., A. Scatena, A. Rosati, R. Giusti, G. Ferro, E. Malagnino, A. Capitanini, A. Piluso, P. Conti, G. Bernabini, et al. 2015. High-volume online haemodiafiltration improves erythropoiesis-stimulating agent (ESA) resistance in comparison with low-flux bicarbonate dialysis: results of the REDERT study. *Nephrol. Dial. Transplant.* 30: 682–689.
9. Budaj, M., Z. Poljak, I. Ďuriš, M. Kaško, R. Imrich, M. Kopáni, L. Maruščáková, and I. Hulín. 2012. Microparticles: a component of various diseases. *Pol. Arch. Med. Wewn.* 122(Suppl. 1): 24–29.
10. Piccin, A., W. G. Murphy, and O. P. Smith. 2007. Circulating microparticles: pathophysiology and clinical implications. *Blood Rev.* 21: 157–171.
11. Camussi, G., M. C. Deregibus, S. Bruno, V. Cantaluppi, and L. Biancone. 2010. Exosomes/microvesicles as a mechanism of cell-to-cell communication. *Kidney Int.* 78: 838–848.
12. Dellepiane, S., D. Medica, A. D. Quercia, and V. Cantaluppi. 2017. The exciting "bench to bedside" journey of cell therapies for acute kidney injury and renal transplantation. [Published erratum appears in 2017 *J. Nephrol.* 30: 337–338.] *J. Nephrol.* 30: 319–336.
13. Hunter, M. P., N. Ismail, X. Zhang, B. D. Aguda, E. J. Lee, L. Yu, T. Xiao, J. Schafer, M.-L. T. Lee, T. D. Schmittgen, et al. 2008. Detection of microRNA expression in human peripheral blood microvesicles. [Published erratum appears in 2010 *PLoS One* 5.] *PLoS One* 3: e3694.
14. Fleury, A., M. C. Martinez, and S. Le Lay. 2014. Extracellular vesicles as therapeutic tools in cardiovascular diseases. *Front. Immunol.* 5: 370.
15. Revenfeld, A. L. S., R. Bæk, M. H. Nielsen, A. Stensballe, K. Varming, and M. Jørgensen. 2014. Diagnostic and prognostic potential of extracellular vesicles in peripheral blood. *Clin. Ther.* 36: 830–846.
16. Zhu, H., and G.-C. Fan. 2011. Extracellular/circulating microRNAs and their potential role in cardiovascular disease. *Am. J. Cardiovasc. Dis.* 1: 138–149.
17. Fichtlscherer, S., A. M. Zeiher, and S. Dimmeler. 2011. Circulating microRNAs: biomarkers or mediators of cardiovascular diseases? *Arterioscler. Thromb. Vasc. Biol.* 31: 2383–2390.
18. Boulanger, C. M., N. Amabile, and A. Tedgui. 2006. Circulating microparticles: a potential prognostic marker for atherosclerotic vascular disease. *Hypertension* 48: 180–186.
19. Burton, J. O., H. A. Hamali, R. Singh, N. Abbasian, R. Parsons, A. K. Patel, A. H. Goodall, and N. J. Brunskill. 2013. Elevated levels of procoagulant plasma microvesicles in dialysis patients. *PLoS One* 8: e72663.
20. Azienda Ospedaliera Città della Salute e della Scienza di Torino. 2017. Effect of mixed on-line hemodiafiltration on circulating markers of inflammation and vascular dysfunction. In ClinicalTrials.gov. National Library of Medicine (US), Bethesda, MD. NLM Identifier: NCT03202212. Available at: https://clinicaltrials.gov/ct2/show/NCT03202212. Accessed: February 16, 2019.
21. Pedrini, L. A., V. De Cristofaro, B. Pagliari, and F. Samà. 2000. Mixed predilution and postdilution online hemodiafiltration compared with the traditional infusion modes. *Kidney Int.* 58: 2155–2165.
22. Figliolini, F., V. Cantaluppi, M. De Lena, S. Beltramo, R. Romagnoli, M. Salizzoni, R. Melzi, R. Nano, L. Piemonti, C. Tetta, et al. 2014. Isolation, characterization and potential role in beta cell-endothelium cross-talk of extracellular vesicles released from human pancreatic islets. *PLoS One* 9: e102521.
23. Campean, V., D. Neureiter, B. Nonnast-Daniel, C. Garlichs, M.-L. Gross, and K. Amann. 2007. CD40-CD154 expression in calcified and non-calcified coronary lesions of patients with chronic renal failure. *Atherosclerosis* 190: 156–166.
24. Afek, A., D. Harats, A. Roth, G. Keren, and J. George. 2005. A functional role for inducible costimulator (ICOS) in atherosclerosis. *Atherosclerosis* 183: 57–63.
25. Migliori, M., V. Cantaluppi, C. Mannari, A. A. E. Bertelli, D. Medica, A. D. Quercia, V. Navarro, A. Scatena, L. Giovannini, L. Biancone, and V. Panichi. 2015. Caffeic acid, a phenol found in white wine, modulates endothelial nitric oxide production and protects from oxidative stress-associated endothelial cell injury. *PLoS One* 10: e0117530.
26. Niwa, T. 2013. Removal of protein-bound uraemic toxins by haemodialysis. *Blood Purif.* 35(Suppl. 2): 20–25.
27. Yamamoto, S., J. J. Kazama, T. Wakamatsu, Y. Takahashi, Y. Kaneko, S. Goto, and I. Narita. 2016. Removal of uremic toxins by renal replacement therapies: a review of current progress and future perspectives. *Ren. Replace. Ther.* 2: 43.
28. Shroff, R. C., R. McNair, N. Figg, J. N. Skepper, L. Schurgers, A. Gupta, M. Hiorns, A. E. Donald, J. Deanfield, L. Rees, and C. M. Shanahan. 2008. Dialysis accelerates medial vascular calcification in part by triggering smooth muscle cell apoptosis. *Circulation* 118: 1748–1757.
29. Jankowski, J., J. Hagemann, M. S. Yoon, M. van der Giet, N. Stephan, W. Zidek, H. Schlüter, and M. Tepel. 2001. Increased vascular growth in hemodialysis patients induced by platelet-derived diadenosine polyphosphates. *Kidney Int.* 59: 1134–1141.
30. Chen, X.-D., M. Deng, J.-S. Zhou, Y.-Z. Xiao, X.-S. Zhou, C.-C. Zhang, M. Wu, Z.-D. Wang, and X.-T. Chen. 2015. Bone Morphogenetic Protein-2 regulates in vitro osteogenic differentiation of mouse adipose derived stem cells. *Eur. Rev. Med. Pharmacol. Sci.* 19: 2048–2053.
31. Li, S., H. Chen, J. Ren, Q. Geng, J. Song, C. Lee, C. Cao, J. Zhang, and N. Xu. 2014. MicroRNA-223 inhibits tissue factor expression in vascular endothelial cells. *Atherosclerosis* 237: 514–520.
32. Yigit, I. P., H. Celiker, A. Dogukan, N. Ilhan, A. Gurel, R. Ulu, and B. Aygen. 2015. Can serum NGAL levels be used as an inflammation marker on hemodialysis patients with permanent catheter? *Ren. Fail.* 37: 77–82.
33. Cantaluppi, V., S. Dellepiane, M. Tamagnone, D. Medica, F. Figliolini, M. Messina, A. M. Manzione, M. Gai, G. Tognarelli, A. Ranghino, et al. 2015. Neutrophil gelatinase associated lipocalin is an early and accurate biomarker of graft function and tissue regeneration in kidney transplantation from extended criteria donors. *PLoS One* 10: e0129279.
34. Canaud, B., J. L. Bragg-Gresham, M. R. Marshall, S. Desmeules, B. W. Gillespie, T. Depner, P. Klassen, and F. K. Port. 2006. Mortality risk for patients receiving hemodiafiltration versus hemodialysis: european results from the DOPPS. *Kidney Int.* 69: 2087–2093.
35. Merello Godino, J. I., R. Rentero, G. Orlandini, D. Marcelli, and C. Ronco. 2002. Results from EuCliD (european clinical dialysis database): impact of shifting treatment modality. *Int. J. Artif. Organs* 25: 1049–1060.

36. Canaud, B., C. Barbieri, D. Marcelli, F. Bellocchio, S. Bowry, F. Mari, C. Amato, and E. Gatti. 2015. Optimal convection volume for improving patient outcomes in an international incident dialysis cohort treated with online hemodiafiltration. *Kidney Int.* 88: 1108–1116.
37. de Sequera, P., M. Albalate, R. Pérez-García, E. Corchete, M. Puerta, M. Ortega, R. Alcázar, T. Talaván, and M. J. Ruiz-Álvarez. 2013. A comparison of the effectiveness of two online haemodiafiltration modalities: mixed versus post-dilution. *Nefrologia* 33: 779–787.
38. Cantaluppi, V., D. Medica, C. Mannari, G. Stiaccini, F. Figliolini, S. Dellepiane, A. D. Quercia, M. Migliori, V. Panichi, L. Giovannini, et al. 2015. Endothelial progenitor cell-derived extracellular vesicles protect from complement-mediated mesangial injury in experimental anti-Thy1.1 glomerulonephritis. *Nephrol. Dial. Transplant.* 30: 410–422.
39. Clement, M., K. Guedj, F. Andreata, M. Morvan, L. Bey, J. Khallou-Laschet, A.-T. Gaston ,S. Delbosc, J.-M. Alsac, P. Bruneval, et al. 2015. Control of the T follicular helper-germinal center B-cell axis by $CD8^+$ regulatory T cells limits atherosclerosis and tertiary lymphoid organ development. *Circulation* 131: 560–570.
40. Packard, R. R. S., and P. Libby. 2008. Inflammation in atherosclerosis: from vascular biology to biomarker discovery and risk prediction. *Clin. Chem.* 54: 24–38.
41. Gerdes, N., and A. Zirlik. 2011. Co-stimulatory molecules in and beyond co-stimulation - tipping the balance in atherosclerosis? *Thromb. Haemost.* 106: 804–813.
42. Desideri, G., V. Panichi, S. Paoletti, D. Grassi, R. Bigazzi, S. Beati, G. Bernabini, A. Rosati, C. Ferri, S. Taddei, and L. Ghiadoni, RISCAVID investigators. 2011. Soluble CD40 ligand is predictive of combined cardiovascular morbidity and mortality in patients on haemodialysis at a relatively short-term follow-up. *Nephrol. Dial. Transplant.* 26: 2983–2988.
43. Cantaluppi, V., A. D. Quercia, S. Dellepiane, S. Ferrario, G. Camussi, and L. Biancone. 2014. Interaction between systemic inflammation and renal tubular epithelial cells. *Nephrol. Dial. Transplant.* 29: 2004–2011.
44. Dellepiane, S., M. Marengo, and V. Cantaluppi. 2016. Detrimental cross-talk between sepsis and acute kidney injury: new pathogenic mechanisms, early biomarkers and targeted therapies. *Crit. Care* 20: 61.
45. Taïbi, F., V. Metzinger-Le Meuth, E. M'Baya-Moutoula, M. s. Djelouat, L. Louvet, J. M. Bugnicourt, S. Poirot, A. Bengrine, J. M. Chillon, Z. A. Massy, and L. Metzinger. 2014. Possible involvement of microRNAs in vascular damage in experimental chronic kidney disease. *Biochim. Biophys. Acta* 1842: 88–98.
46. Taïbi, F., V. Metzinger-Le Meuth, Z. A. Massy, and L. Metzinger. 2014. miR-223: an inflammatory oncomiR enters the cardiovascular field. *Biochim. Biophys. Acta* 1842: 1001–1009.
47. Wang, Y., Y. Zhang, J. Huang, X. Chen, X. Gu, Y. Wang, L. Zeng, and G.-Y. Yang. 2014. Increase of circulating miR-223 and insulin-like growth factor-1 is associated with the pathogenesis of acute ischemic stroke in patients. *BMC Neurol.* 14: 77.
48. Dai, G.-H., P.-Z. Ma, X.-B. Song, N. Liu, T. Zhang, and B. Wu. 2014. MicroRNA-223-3p inhibits the angiogenesis of ischemic cardiac microvascular endothelial cells via affecting RPS6KB1/hif-1a signal pathway. *PLoS One* 9: e108468.
49. Wang, Y.-S., J. Zhou, K. Hong, X.-S. Cheng, and Y.-G. Li. 2015. MicroRNA-223 displays a protective role against cardiomyocyte hypertrophy by targeting cardiac troponin I-interacting kinase. *Cell. Physiol. Biochem.* 35: 1546–1556.
50. Shrestha, K., A. G. Borowski, R. W. Troughton, A. L. Klein, and W. H. W. Tang. 2012. Association between systemic neutrophil gelatinase-associated lipocalin and anemia, relative hypochromia, and inflammation in chronic systolic heart failure. *Congest. Heart Fail.* 18: 239–244.
51. Rangrez, A. Y., E. M'Baya-Moutoula, V. Metzinger-Le Meuth, L. Hénaut, M. S. Djelouat, J. Benchitrit, Z. A. Massy, and L. Metzinger. 2012. Inorganic phosphate accelerates the migration of vascular smooth muscle cells: evidence for the involvement of miR-223. *PLoS One* 7: e47807.
52. M'Baya-Moutoula, E., L. Louvet, V. Metzinger-Le Meuth, Z. A. Massy, and L. Metzinger. 2015. High inorganic phosphate concentration inhibits osteoclastogenesis by modulating miR-223. *Biochim. Biophys. Acta* 1852(10 Pt A): 2202–2212.